Food & Function

Accepted Manuscript

This article can be cited before page numbers have been issued, to do this please use: P. D. D. F. Santos, C. R. L. Francisco, A. Coqueiro, F. V. Leimann, J. Pinela, R. C. Calhelha, R. Porto Ineu, I. C. F. R. Ferreira, E. Bona and O. H. Gonçalves, *Food Funct.*, 2019, DOI: 10.1039/C8FO02431F.

ROYAL SOCIETY OF CHEMISTRY

rsc.li/food-function

View Article Online
DOI: 10.1039/C8FO02431F

Nanoencapsulation of curcuminoids extracted from *Curcuma longa* L. and evaluation of cytotoxic, enzymatic, antioxidant and anti-inflammatory activities

Priscila Dayane Freitas dos Santos[a], Cristhian Rafael Lopes Francisco[b], Aline Coqueiro[a], Fernanda Vitória Leimann[a,c,d], José Pinela[d], Ricardo C. Calhelha[d], Rafael Porto Ineu[a], Isabel C.F.R. Ferreira[d] *, Evandro Bona[a], Odinei Hess Gonçalves[a,c,d]

[a]Post-Graduation Program of Food Technology (PPGTA), Federal University of Technology – Paraná – UTFPR, Campus Campo Mourão, via Rosalina Maria dos Santos, 1233, CEP 87301-899, Caixa Postal: 271, Campo Mourão, PR, Brazil.

[b]Food Department (DALIM), Federal University of Technology – Paraná – UTFPR, Campus Campo Mourão, via Rosalina Maria dos Santos, 1233, CEP 87301-899, Caixa Postal: 271, Campo Mourão, PR, Brazil.

[c]Laboratory of Separation and Reaction Engineering - Laboratory of Catalysis and Materials (LSRE-LCM), Polytechnic Institute of Bragança, Campus de Santa Apolónia, 5300-253 Bragança, Portugal.

[d]Centro de Investigação de Montanha (CIMO), Instituto Politécnico de Bragança, Campus de Santa Apolónia, 5300-253 Bragança, Portugal.

**Corresponding author: iferreira@ipb.pt*

ABSTRACT

View Article Online
DOI: 10.1039/C8FO02431F

Curcumin, bisdemethoxycurcumin and demethoxycurcumin are the main curcuminoids present in *Curcuma longa* L. and are known for their bioactivity. However, their low water solubility results in poor bioavailability and therapeutic efficacy. This work aimed to investigate the *in vitro* modulation capacity on the enzymes acetylcholinesterase (AChE) and glutathione S-transferase (GST), as well as the *in vitro* antioxidant (OxHLIA and TBARS) and anti-inflammatory activities (RAW 264.7 test) of nanoencapsulated curcuminoids. Cytotoxicity on tumor and non-tumor cell lines was also investigated. Curcuminoids nanoparticles significantly inhibited the *in vitro* activity of AChE (12% inhibition at 50 μM) and GST (30% inhibition at 5 μM). They presented antioxidant activity and toxic effects against breast adenocarcinoma, lung, cervical and hepatocellular carcinoma cells when dispersed in water. Encapsulated curcuminoids exhibited bioactive properties in aqueous medium (no hydrophobic solvent added), exerting antioxidant and cytotoxic effects and acting on the cholinergic and endogenous antioxidant systems.

Keywords: curcumin; nanoparticles; reactive oxygen species, solid dispersion; cholinergic system.

1. Introduction

Acetylcholine (ACh) is a neurotransmitter involved in cognitive functions, such as memory, and acetylcholinesterase (AChE - E.C. 3.1.1.7) is the main enzyme associated with ACh hydrolysis during the cholinergic cycle, balancing the concentration of this neurotransmitter in the synaptic cleft.[1,2] According to the

View Article Online
DOI: 10.1039/C8FO02431F

cholinergic hypothesis, the Alzheimer's disease is related to imbalances in the cholinergic system, which occur due to a reduction in ACh amount. The ultimate effect is the difficulty in the propagation of information between neurons leading to cognitive impairment. [3]

Oxidative stress is another condition that may lead to several health issues. It occurs due to an imbalance between endogenous antioxidants and reactive species, which are naturally produced in the human body. Reactive oxygen species (ROS), such as superoxide radical ($O_2^{\cdot-}$) and hydrogen peroxide (H_2O_2), are formed during cellular processes, including cellular respiration.[4,5] An excess in ROS amounts may cause oxidation of cellular components, such as lipids from cell membranes, resulting in tissues damage and allowing the promotion of conditions such as cancer, diabetes, neurological and cardiovascular diseases, among others.[6–10] In order to avoid ROS damage, the human body possesses an antioxidant defense system including enzymes such as superoxide dismutase (SOD - E.C. 1.15.1.1), catalase (CAT - E.C. 1.11.1.6) and glutathione S-transferase (GST - E.C. 2.5.1.18), besides non-enzymatic antioxidants, such as reduced glutathione (GSH). SOD is responsible for dismuting superoxide radicals in oxygen and hydrogen peroxide, and then CAT catalyzes hydrogen peroxide conversion into oxygen and water. GST stabilizes electrophiles by catalyzing their conjugation with GSH. [7,11,12]

Some compounds are able to modulate or even mimic enzymes action, allowing to control enzymatic systems and, in this case, avoiding or reversing memory loss and oxidative stress. These substances may be synthetic drugs such as donepezil, rivastigmine, galantamine and ethacrynic acid, or natural substances such as flavonoids and carotenoids. [13–17] Bisdemethoxycurcumin,

View Article Online
DOI: 10.1039/C8FO02431F

demethoxycurcumin and curcumin are the most abundant curcuminoids found in the rhizomes of turmeric (*Curcuma longa* L.) and present several interesting properties such as antioxidant, [18] antimicrobial, [19,20] anti-inflammatory, [21,22] immunomodulatory [23] and anticancer. [24]

Studies have also shown that curcuminoids may act as modulators of cholinergic and antioxidant enzymes. Ahmed and Gilani [25] showed that both individual and total curcuminoids were able to inhibit *in vitro* and *ex vivo* activity of AChE in rats. However, authors showed that curcumin modulated enzymatic activity only in memory assays and that the three curcuminoids together are more efficient on enhancing ACh levels in the body. Jaques and co-workers [26] demonstrated that rats exposed to cigarette smoke presented increase in the levels of AChE from cerebral cortex. In rats treated with curcumin this increase was not observed, meaning that curcumin was able to modulate the cholinergic system. Abbasi and co-workers [27] found that curcumin and its synthetic derivatives inhibited AChE activity, with IC_{50} values ranging from 58 to 298 μmol.L^{-1}.

Using an experimental model in which oxidative damage was induced by arsenic in rats, Sankar and co-workers [28] verified that free and encapsulated curcumin reversed the inhibition of antioxidant enzymes SOD, CAT, glutathione peroxidase (GPx - E.C. 1.11.1.9) and glutathione reductase (GR - E.C. 1.8.1.7). Van Iersel and co-workers [16] showed that curcumin at 25 μM inhibited 96% of GST activity from human melanoma cells. Exposition of rats to carbofuran resulted in inhibition of enzymes SOD, GST and CAT, but treatment with curcumin attenuated this inhibition [29]. Panahi et al. [30] found that curcuminoids-piperine supplementation increased the serum SOD activity in subjects with

View Article Online
DOI: 10.1039/C8FO02431F

metabolic syndrome. Besides modulating activity of endogenous antioxidant enzymes, curcuminoids may act directly as antioxidants, protecting cells, such as erythrocytes, from the damages caused by oxidizing agents. It was demonstrated that curcumin and its synthetic analogues attenuated the free radical-induced oxidative hemolysis of human red blood cells, with 10 μM curcumin protecting 50% of erythrocytes for 240 min. [31]

It is known that curcuminoids present low bioavailability which is often related to their high hydrophobicity. Encapsulation is a promising alternative to avoid the technological drawbacks of curcuminoids and the solid dispersion technique has been applied to various drugs and natural bioactive substances. [32–34] Although curcuminoids bioactivity is well described in the literature, it is important to determined how encapsulation may affect their properties.

The objective of this work was to determine the influence of curcuminoids-loaded nanoparticles on the modulation of the AChE and GST *in vitro* enzymatic activity, their cytotoxicity against human tumor cell lines (MCF-7, NCI-H460, HeLa and HepG2) and a non-tumor cell line (PLP2), and their protective effect on lipid peroxidation and oxidative hemolysis.

2. Material and methods

2.1 Plant material, standards and reagents

Curcuma longa L. rhizomes were acquired in the local market in Campo Mourão, Paraná, Brazil. Ethanol (99.8%, Neon) and polyvinylpyrrolidone (40.000 $g.mol^{-1}$, Sigma-Aldrich) were used on the extraction and encapsulation

View Article Online
DOI: 10.1039/C8FO02431F

of the curcuminoids. Commercial curcumin (81.9 ± 2.4 % curcumin, 15.8 ± 0.5 % demethoxycurcumin and 2.3 ± 0.1 % bisdemethoxycurcumin, chromatogram presented in Supplementary Material, Figure S1) was used in the characterization of nanoparticles. Chromatographic standards of curcumin, demethoxycurcumin and bisdemethoxycurcumin were purchased from Sigma-Aldrich. Dibasic potassium phosphate (Neon), tris(hydroxymethyl)aminomethane (Dinâmica), monobasic potassium phosphate (Vetec), L-glutathione (Vetec), 1-chloro-2,4-dinitrobenzene (CDNB, Sigma-Aldrich), 5,5′-dithiobis(2-nitrobenzoic acid) (DTNB) (> 98%, Sigma-Aldrich) and acetylthiocholine iodide (> 98%, Sigma-Aldrich) were used in the enzymatic assays. Wistar rat brain tissue were provided by State University of Maringá (UEM) for the enzymatic analyses. Acetic acid, sulforhodamine B (SRB), ellipticine, trypan blue, trichloroacetic acid (TCA), lipopolysaccharide (LPS), 6-hydroxy-2,5,7,8-tetramethylchroman-2-carboxylic acid (Trolox), 2,2'-azobis(2-methylpropionamidine) dihydrochloride (AAPH) and tris-(hydroxymethyl)aminomethane (TRIS) were purchased from Sigma (St Louis, MO, USA). Dimethyl sulfoxide (DMSO) was acquired from Fisher Scientific (Lisbon, Portugal). Dulbecco's Modified Eagle's Medium (DMEM) and RPMI-1640 medium, fetal bovine serum (FBS), Hank's balanced salt solution (HBSS), L-glutamine, nonessential amino acid solution (2 mM), penicillin/streptomycin solution (100 U mL^{-1} and 100 mg mL^{-1}, respectively), trypsin, and EDTA were acquired from Hyclone (Logan, UT, USA). All other chemicals were purchased from common sources. For the cytotoxicity and antioxidant activity assays, water was treated in a Milli-Q water purification system (TGI Pure Water Systems, USA) before use.

View Article Online
DOI: 10.1039/C8FO02431F

2.2 Curcuminoids nanoparticles production

Curcumin nanoparticles were produced using a simultaneous extraction and encapsulation procedure based on the work of Rocha et al. [35] Briefly, *Curcuma longa* rhizomes were freeze-dried, milled and the particles with sizes from 150 to 425 µm were selected for the extraction/encapsulation. Polyvinylpyrrolidone (PVP, 15.38 mg) was dissolved in 10 mL of 99% ethanol in water under magnetic stirring. This solution was then poured into a Falcon tube containing turmeric powder (10 mg), and the mixture was sonicated for 3 min in a pulse regime (30 s on and 10 s off) at 29.9 °C. After that, the dispersion was filtered (0.45 µm) and dried in a circulation oven at 60 °C. Finally, nanoparticles were stored at 10 °C protected from light. The same procedure was applied without the use of PVP in order to obtain the free curcuminoids used in the biological assays.

2.3 Nanoparticles characterization

Curcuminoids were quantified by High Performance Liquid Chromatography (HPLC, Dionex – UltiMate 3000) using the external calibration technique. Calibration curves were obtained for each curcuminoid standards (curcumin, demethoxycurcumin and bisdemethoxycurcumin). Acetonitrile and acidified water (1% v/v acetic acid) were used as mobile phase at 1 $mL.min^{-1}$, in an Acclaim® 120 C18 column (4,6 x 250 mm and particle size of 5 µm, Dionex-Thermo Scientific) at 40 °C. The elution gradient went from 60% to 100% acetonitrile in 8 min, remaining in this composition for 4 min before returning to the initial condition. Detection was performed by a diode array detector (DAD) at 427 nm.

An aliquot of the nanoparticles dispersion (2 mL) was transferred to a test tube and kept in a circulation oven at 60 °C until solvent evaporation. After that, distilled water was added to the tube (4 mL) and it was maintained at 25 °C for 3 h. The obtained solution was filtered through syringe filter (0.45 μm porosity), frozen at -80°C and freeze-dried (Liotop, L101). The sample was then dissolved in methanol and its concentration was determined by HPLC. The colloidally stable curcuminoids fraction (CSC, $\mu g.mg_{turmeric}^{-1}$) was considered to be the one that passed through the filter (fraction formed by nanoparticles with diameters smaller than 450 nm), calculated by Equation 1 where C_{cur} is the curcuminoid concentration determined by HPLC ($\mu g.mL^{-1}$), $V_{solvent}$ is the methanol volume added to freeze-dried sample (mL) and $m_{turmeric}$ is the turmeric mass used in the process (mg).

$$CSC = \frac{C_{cur} \times V_{solvent}}{m_{turmeric}} \quad (1)$$

Thermal properties of curcuminoids-loaded nanoparticles were determined by Differential Scanning Calorimetry (DSC, Perkin Elmer DSC4000). Nanoparticles, pure compounds (curcumin and PVP) and their physical mixture (curcumin/PVP ratio of 1:15 wt/wt manually mixed) were weighed (3 to 5 mg) in aluminum pans. Samples were heated from 20 to 200 °C at 20 $°C.min^{-1}$ under nitrogen flow of 50 $mL.min^{-1}$. Fourier Transform Infrared Spectroscopy (FTIR, Shimadzu Affinity-1) was performed from 4000 to 600 cm^{-1}, with 2 cm^{-1} resolution and 32 cumulative scans in order to identify chemical interactions between curcuminoids and PVP. Nanoparticles morphology was evaluated by Transmission Electron Microscopy (TEM, JEOL JEM-1011, 100 kV). Drops of

View Article Online
DOI: 10.1039/C8FO02431F

each sample were deposited onto 300 *mesh* parlodium-coated copper grids and dried under room temperature and then analyzed. X-Ray Diffraction analysis (Bruker, D8 advance) was carried out to reveal changes in the crystalline structure of curcuminoids after the encapsulation process. The following conditions were used: angular interval of 3 to 60°, angular speed of 5,9°.min^{-1}, 40 KW and 35 mA.

2.4 Biological assays

2.4.1 Brain tissues preparation

Rat brains were weighed and homogenized in 10 volumes of 10 mM Tris-HCl buffer (pH 7.4), at 12,000 rpm for 1 min (Ultra-turrax, IKA T25 digital). After that, homogenates were centrifuged at 9700xg for 10 min (MiniSpin plus, Eppendorf) and supernatants (S1) were stored at -80 °C. For the enzymatic analyzes, curcuminoids and curcuminoids-loaded nanoparticles doses were defined according to previous concentration curves (from 25 µM to 200 µM for acetylcholinesterase (AChE - E.C. 3.1.1.7) and from 0,01 µM to 200 µM for glutathione S-transferase (GST - E.C. 2.5.1.18)).

2.4.2 *In vitro* acetylcholinesterase (AChE) assay

AChE activity was assessed according to the method described by Ellman et al. [36] with minor adaptations. The method is based on the hydrolysis of acetylthiocholine by AChE, followed by the reaction of thiocholine (hydrolysis product) with DTNB, resulting in a yellow colored compound (TNB). Mixtures consisting of 1.04 mM 5,5′-dithiobis(2-nitrobenzioc) acid (DTNB), 24 mM

View Article Online
DOI: 10.1039/C8FO02431F

potassium phosphate buffer (pH 7.5), S1 and test compound solution were pre-incubated at 25 °C for 2 min. Then, 0.83 mM of acetylthiocholine was added and the reaction was measured during 4 min in a UV-Vis spectrophotometer (OceanOptics, USB650) at 480 nm (due to the maximum absorbance of curcumin at 427 nm). The following samples were test: curcuminoids-loaded nanoparticles in water and free curcuminoids in DMSO 3.33%, both in the final concentrations of 25 μM, 50 μM, 100 μM and 200 μM; PVP in water in the final concentration of 13.8 μM (which corresponds to the PVP amount in 100 μM solution of nanoparticles); and free curcuminoids at 200 μM in water. Results were expressed as percent of enzyme activity in comparison to control (mixture without test compound solution).

2.4.3 *In vitro* glutathione S-transferase assay

GST activity was assessed according to the method described by Habig, Pabst and Jakoby. [37] Mixtures consisting of 24 mM potassium phosphate buffer (pH 7.5), S1 and test compound solution were pre-incubated at 25 °C for 2 min, and the mixed with 1 mM 1-chloro-2,4-dinitrobenzene (CDNB) and 1 mM reduced glutathione (GSH). Enzymatic activity was measured during 4 min in a UV-Vis spectrophotometer (OceanOptics, USB650) at 340 nm. The following samples were tested: curcuminoids nanoparticles in water (0.1 μM, 5 μM, 25 μM and 50 μM); free curcuminoids in DMSO 3.33% (of 5 μM, 25 μM and 50 μM); PVP in water in the final concentration of 13.8 μM (which corresponds to the PVP amount in 100 μM solution of nanoparticles); and free curcuminoids in water at 50 μM. Results were expressed as percent of enzyme activity in comparison to control (mixture without test compound solution).

View Article Online
DOI: 10.1039/C8FO02431F

2.4.4 Oxidative hemolysis inhibition assay (OxHLIA)

The antihemolytic activity was assessed according to the method described by Lockowandt et al. [38] Sheep blood samples were collected from healthy animals and centrifuged at 1,000xg for 5 min at 10 ºC. Plasma and buffy coats were discarded and erythrocytes were first washed once with NaCl (150 mM) and three times with phosphate-buffered saline (PBS, pH 7.4). [39] The erythrocyte pellet was then resuspended in PBS at 2.8% (v/v). Using a flat bottom 48-well microplate, 200 µL of erythrocyte solution was mixed with 400 µL of either PBS solution (control), free and nanoencapsulated curcuminoids dissolved in PBS, or water (for complete hemolysis). Trolox was used as a positive control. After pre-incubation at 37 ºC for 10 min with shaking, AAPH (200 µL, 160 mM in PBS) was added and the optical density was measured in a microplate reader (Bio-Tek Instruments, ELX800) at 690 nm. After that, the microplate was incubated under the same conditions and the optical density was measured every 10 min at the same wavelength for approximately 400 min. The percentage of the erythrocyte population that remained intact (*P*) was calculated using Equation 2:

$$P(\%) = \left(\frac{S_t - CH_0}{S_t - CH_0}\right) \qquad (2)$$

where S_t and S_0 correspond to the optical density of the sample at *t* and 0 min, respectively, and CH_0 is the optical density of the complete hemolysis at 0 min. Results were expressed as delayed time of hemolysis (Δt), which was calculated using Equation 3:

$$\Delta t \text{ (min)} = Ht_{50} \text{ (sample)} - Ht_{50} \text{ (control)} \qquad (3)$$

View Article Online
DOI: 10.1039/C8FO02431F

where Ht_{50} is the 50% hemolytic time (min) graphically obtained from the hemolysis curve of each sample concentration. The Δt values were then correlated to the different compound concentrations and, from the obtained correlation, the concentration able to promote a Δt haemolysis delay was calculated. Results were expressed as IC_{50} values ($\mu g.mL^{-1}$) at Δt 60 and 120 min, i.e., compound concentration required to keep 50% of the erythrocyte population intact for 60 and 120 min.

2.4.5 TBARS formation inhibition assay

The capacity of the free and nanoencapsulated curcuminoids to inhibit the formation of thiobarbituric acid reactive substances (TBARS), such as malondialdehyde generated from the *ex vivo* decomposition of lipid peroxidation products, was evaluated using porcine brain cell homogenates, following the method described previously by Pinela et al. [40] Trolox was used as positive control. Results were expressed as IC_{50} values ($\mu g.mL^{-1}$), i.e., compound concentration providing 50% of antioxidant activity.

2.4.6 Anti-inflammatory activity assay

The lipopolysaccharide (LPS)-induced nitric oxide (NO) production by a murine macrophage (RAW 264.7) cell line was determined as nitrite concentration in the culture medium according to the method described by Sobral et al. [41] The effect of the tested compounds in the absence of LPS was also evaluated, in order to observe if they induced changes in NO basal levels. In

View Article Online
DOI: 10.1039/C8FO02431F

negative controls, no LPS was added. For the NO determination, a Griess Reagent System kit containing sulfanilamide, N-1-naphthylethylenediamine dihydrochloride (NED) and nitrite solutions was used. Dexamethasone was used as a positive control. Results were expressed as IC_{50} values ($\mu g.mL^{-1}$), i.e. compound concentration providing 50% of NO production inhibition.

2.4.7 Cytotoxicity assay

The sulforhodamine (SRB) assay was performed to assess the cytotoxicity of free and nanoencapsulated curcuminoids, according to a procedure previously described by Abreu and co-workers. [42] Free curcuminoids were dissolved in a DMSO/water mixture (1:1, v/v) at 8 $mg.L^{-1}$, since the compounds are insoluble in water. Curcuminoids nanoparticles were dispersed in water at the same concentration. Successive dilutions were prepared from the stock solutions. MCF-7 (breast adenocarcinoma), NCI-H460 (non-small cell lung carcinoma), HeLa (cervical carcinoma) and HepG2 (hepatocellular carcinoma) from DSMZ (Leibniz-Institute DSMZ - German Collection of Microorganisms and Cell Cultures) normal cells, were selected as human tumor cell lines. To evaluate the toxicity against normal cells, a primary porcine liver (PLP2) cell culture was prepared according to a method established by Abreu et al. (2011). These cells were treated for 48 h with the different sample solutions and then submitted to the SRB assay. Ellipticine was used as a positive control. Results were expressed as GI_{50} values, i.e. compound concentration providing 50% of net cell growth inhibition.

View Article Online
DOI: 10.1039/C8FO02431F

2.5 Statistical analysis

Statistical analyses of AChE and GST activity were carried out using Graph Pad Prism 6.0 software (Graph Pad, USA) and significance between groups was assessed by one-way analysis of variance (ANOVA) followed by Tukey *post hoc* tests when appropriate. Results were expressed as mean ± standard error of mean (SEM) and *p*-values lower than 0.05 were considered to be indicative of significance. Results of antioxidant, anti-inflammatory and cytotoxic activities were analyzed using SPSS Statistics software (IBM SPSS Statistics for Windows, Version 22.0. Armonk, NY: IBM Corp.) and differences among the two samples was assessed applying a two-tailed paired Student's t-test at a 5% significance level. Results were expressed as mean ± standard deviation.

3. Results and discussion

3.1 Curcuminoids-PVP nanoparticles characterization

Figures 1 presents the chromatogram of the curcuminoids nanoparticles as well as the FTIR spectra, DSC thermograms and DRX patterns of curcumin, PVP, physical mixture (curcumin/PVP ratio of 1:15 wt/wt manually mixed and at 1:1 wt:wt when indicated) and curcuminoids nanoparticles. A Transmission Electron Microscopy image of the nanoparticles is presented in Figure 2.

Figure 1

Figure 2

Nanometric particles were formed with spherical morphology as one may see in the TEM image. HPLC showed that the curcuminoids fractions in the

View Article Online
DOI: 10.1039/C8FO02431F

nanoparticles were composed of 56.6 ± 0.2 % curcumin, 21.3 ± 0.1 % demethoxycurcumin and 22.1 ± 0.1 % bisdemethoxycurcumin. Colloidally stable fraction found were curcuminoids were (in $\mu g.mg_{turmeric}^{-1}$) 2.71 ± 0.36 for curcumin, 1.04 ± 0.13 for demethoxycurcumin and 1.11 ± 0.12 for bisdemethoxycurcumin. This increase in water affinity was probably caused by the interactions between the curcuminoids and PVP, since its amphiphilic feature allows the formation of a soluble complex that stabilizes curcuminoids in water. [43,44] Karavas and co-workers [34] verified that felodipine solubility increased until a maximum of 16 $mg.L^{-1}$ as PVP concentration increased. However, for high PVP concentration the increase was not significant. Silva et al. [45] encapsulated lutein into PVP and showed that interactions between the compounds become more important as PVP concentration was elevated.

Characteristic absorption peaks of curcumin were observed at 3513 cm^{-1} (OH stretching vibration), 1629 cm^{-1} (carbonyl group (C=O)), 1602 cm^{-1} (aromatic ring stretching vibration), 1512 cm^{-1} (C=C bonds), 1428 cm^{-1} (C–H bending vibration), 1283 cm^{-1} (aromatic C–O stretching) and 1027 cm^{-1} (C–O–C stretching vibration). [46–48] PVP spectrum showed a broad peak between 3700 and 3000 cm^{-1}, which is attributed to the presence of residual moisture in the material, a second broad peak at about 3000 and 2800 cm^{-1}, indicating stretching vibration of asymmetric C–H, and a band ranging from 1800 to 1540 cm^{-1}, assigned to carbonyl stretching vibration. [49–51] Physical mixture spectrum presented absorption peaks of both pure compounds, differently of the nanoparticles spectrum in which curcumin characteristic peaks, such as OH stretching vibration, were not observed. It strongly suggests the existence of interactions

View Article Online
DOI: 10.1039/C8FO02431F

between curcumin and PVP, probably through hydrogen bonding, and, consequently, its encapsulation into the polymer matrix. [52–54]

Curcumin thermogram presented an endothermic peak at 179.4°C, assigned to its melting point. [55] In the PVP curve, a broad endothermic peak ranging from 32 to 134 °C was observed, which is related to moisture loss since PVP is a highly hygroscopic material. [51] Thermogram of the physical mixture showed the endothermic peaks attributed to both pure compounds, but curcumin melting point was not found in the nanoparticles DSC curve. This fact evidences the change in the physical structure of curcumin from crystalline to amorphous, thus indicating its encapsulation into the PVP matrix. [43,54]

Curcumin diffraction pattern revealed a series of peaks between 8 and 30° characteristic of its crystalline structure. [24,56] PVP pattern did not show any peak, confirming its amorphous nature. Curcumin peaks are observed in the 1:1 wt/wt ratio physical mixture pattern, but are not found in the 1:15 wt/wt ratio diffractogram which represents the same curcumin concentration found in the nanoparticles. This demonstrates that the low curcumin concentration was responsible for the fact that the peaks were not detected.

Despite the low sensitivity of X-ray diffraction to detect the curcumin in the physical mixture, DSC and FTIR strongly suggested that curcumin was entrapped in the PVP matrix in the nanoparticles. These results are corroborated by the increase in water affinity detected by the HPLC analysis.

3.2 Enzymatic modulation activity

View Article Online
DOI: 10.1039/C8FO02431F

Figure 3a shows the effect of curcuminoids and nanoencapsulated curcuminoids on the acetylcholinesterase (AChE) activity. Figure 3b presents GST activity in the presence of free (at 5 μM, 25 μM and 50 μM) and nanoencapsulated curcuminoids (at 0.1 μM, 5 μM, 25 μM and 50 μM).

Figure 3

Free and encapsulated curcuminoids modulated the enzymatic activity in a concentration-dependent behavior and higher concentrations of the compounds led to lower AChE activity (Figure 3a). Curcuminoids started to significantly inhibit the enzyme activity ($p < 0.001$) at 100 μM, resulting in a percent inhibition near 21%. Curcuminoids nanoparticles showed significant inhibition ($p < 0.05$) at 50 μM reducing 12% of the enzyme activity. AChE activity was not significantly affected by PVP in water, which means that the modulatory effect presented by the curcuminoids-loaded nanoparticles was not due to this encapsulant. It is worth noting that the effect of free and encapsulated curcuminoids in water on the AChE activity significantly differed ($p > 0.05$), at the same concentration (200 μM). Curcuminoids in water at 200 μM were not able to inhibit the enzyme activity, showing that the encapsulation process led to the improvement of the curcuminoids modulatory properties, despite their inherent hydrophobicity. Ahmed and Gilani [25] reported that free curcuminoids in ethanol (30 μM) inhibited around 60% of AChE activity. In the present study, the higher inhibition of AChE activity (27%) was achieved at 200 μM of free curcuminoids. Authors used electric eel as enzymatic source, which could explain the difference.

According to the cholinergic hypothesis, neurodegenerative diseases, such as Alzheimer's disease, are caused by loss of acetylcholine neurotransmitters or by increase in AChE activity in the brain. As a result, contact

View Article Online
DOI: 10.1039/C8FO02431F

time between neurotransmitters and post-synaptic membrane receptors is reduced, hindering information transmission through neurons and leading to memory loss. Therefore, usual drugs in neurodegenerative diseases treatment consist of AChE reversible inhibitors, which balance cholinergic system and allow enough time contact for information spread in the nervous system. [17,57,58] In this work, encapsulated curcuminoids acted as AChE reversible inhibitors, suggesting that they could potentially be applied in the treatment of diseases related to cholinergic dysfunction.

Both free and encapsulated curcuminoids presented a concentration-dependent effect on the glutathione S-transferase (GST) activity (Figure 3b). Free curcuminoids significantly ($p < 0.05$) inhibited around 20% of GST activity at 25 μM while curcuminoids-loaded nanoparticles presented 30% significant inhibition ($p < 0.05$) at 5 μM. GST activity was not significantly inhibited by PVP *per se*. Free and encapsulated curcuminoids in water, at the final concentration of 50 μM, presented significantly different behaviors ($p > 0.05$). At this concentration, free curcuminoids in water were not able to inhibit enzymatic activity, while curcuminoids nanoparticles significantly inhibited GST ($p < 0.001$) in approximately 55%.

GST is one of the enzymes acting against oxidative stress inside the human body, detoxifying xenobiotics and cytotoxic agents such as drugs, toxins and carcinogens. Excessive activity of this enzyme is associated with multidrug resistance, a clinical condition usually observed during treatment of diseases such as cancer, which reduces therapy efficiency and partial inhibition of enzymatic activity would be interesting in such cases. [13,59,60] Other authors reported inhibition of GST in rats liver tissue experiments (58% inhibition at 30

View Article Online
DOI: 10.1039/C8FO02431F

μM) [61] and human recombinant GST (50% inhibition at 5 μM). [59] The divergence between results could explained by the fact that these works used pure curcumin instead of curcuminoids and different enzymes sources. In the present work, free and encapsulated curcuminoids inhibited the *in vitro* GST activity, however it is worth noting that significant inhibition occurred in a lower concentration in the case of the encapsulated compounds.

Results evidenced that encapsulated curcuminoids modulated AChE and GST activities in a more efficient way than the free compounds. It may be explained by the hydrophilic nature of curcuminoids-PVP nanoparticles, which could lead to interactions between nanoparticles and water molecules stabilizing the enzyme active site. Moreover, there is evidences that nanoparticles sizes could cause enzyme inhibition by a steric effect. [17,62]

3.2 Antioxidant, anti-inflammatory and cytotoxic activities

Results of cytotoxicity and cell-based antioxidant and anti-inflammatory activities of pure and encapsulated curcuminoids are presented in Table 1.

Table 1

Results of the oxidative hemolysis inhibition assay (OxHLIA) are given as IC_{50} values ($\mu g.mL^{-1}$) at Δt 60 and 120 min, i.e., the extract concentration required to protect 50% of the erythrocyte population (*P*) from the hemolytic action caused by the used oxidizing agent for 60 and 120 min; while the IC_{50} values of TBARS correspond to the extract concentration that provides 50% of antioxidant activity. The lower the IC_{50} values, the higher the antioxidant capacity of the samples. In the OxHLIA assay, the erythrocyte population was subjected to hemolytic action

of hydrophilic and lipophilic radicals in aqueous system. [63] Hydrophilic radicals resulted from the thermal decomposition of AAPH, which is a peroxyl radical initiator that attacks the erythrocyte membranes and eventually causes hemolysis. In turn, lipophilic radicals were generated due to this attack through a lipid peroxidation phenomenon. The TBARS assay provided information on the compounds capacity to inhibit the formation of TBARS, such as malondialdehyde generated from the *ex vivo* decomposition of lipid peroxidation products, in aqueous medium. Curcuminoids showed the highest antioxidant activity, with IC_{50} values of 7.2 ± 0.5 $\mu g.mL^{-1}$ and 15.9 ± 0.4 $\mu g.mL^{-1}$ at 60 and 120 min, respectively, for OxHLIA, and 1.04 ± 0.07 $\mu g.mL^{-1}$ for TBARS. This activity was even greater than that of the used positive control, trolox. Moreover, nanoencapsulated curcuminoids presented activity despite the fact only PBS or water was present (in the OxHLIA and TBARS assays, respectively), meaning that encapsulation improved their activity in aqueous medium. Similar results were described by Hatia et al., [64] who found that hemolysis of half the human erythrocytes was delayed by curcumin (50 μM) from 115 min (in the control) to approximately 600 min.

Both samples presented toxic effects against human tumor cell lines (Table 1). Pure curcuminoids were dispersed in DMSO, otherwise it would not be possible to assess their properties due to the poor water solubility. Thus, free curcuminoids had lower GI_{50} values than curcuminoids nanoparticles, probably due to their higher bioavailability in DMSO. On the other hand, encapsulation allowed curcuminoids to exert cytotoxicity on tumor cells in aqueous medium. The non-tumor cell line (PLP2) was not affected by nanoparticles and the toxic concentration of free curcuminoids in this case was much higher than the required

View Article Online
DOI: 10.1039/C8FO02431F

for tumor cells. In the study conducted by Yoon et al., [65] it was demonstrated that turmeric extract powder at 0.5 mg.mL^{-1} reduced in 60% the cell viability of HepG2 tumor cell line, while the cytotoxic activity of turmeric extract-loaded nanoemulsion powder (in which curcumin proportion was lower) did not differ from the control. Zamrus et al. [66] reported that curcumin dispersed in DMSO presented IC_{50} values of 22.50 and above 30 μg.mL^{-1} against MCF-7 and HeLa tumor cell lines, respectively. In another work, it was evidenced that curcuminoids at 50 μM inhibited almost 60% of MCF-7 human breast cancer cells survival. [67]

RAW 264.7 cells are macrophages that release pro-inflammatory cytokines as a response to the contact with bacterial metabolites, for instance. The overexpression of these cytokines is related to the development of several diseases, including cancer. Compounds with anti-inflammatory activity, such as curcuminoids, are able to inhibit cytokines expression, diminishing inflammatory responses and their effects. [68] In this study, only free curcuminoids in DMSO presented anti-inflammatory action against RAW 264.7 cytokines (Table 1), with an IC_{50} value of 61±3 μg.mL^{-1}.

4. Conclusion

Curcuminoids from turmeric were simultaneously extracted and encapsulated into a polyvinylpyrrolidone (PVP) matrix. Physico-chemical and morphologic characterization evidenced that curcuminoids were efficiently encapsulatated. Nanoencapsulated curcuminoids presented improved inhibition of the *in vitro* activity of acetylcholinesterase (AChE) and glutathione S-transferase (GST) enzymes when compared to free curcuminoids. Moreover, encapsulation allowed curcuminoids to exert their antioxidant and cytotoxic

effects in aqueous medium, unlike the compounds in their hydrophobic original form. This could be accounted for the improved water affinity and the reduced size of the nanoparticles.

Acknowledgements

Authors thank CNPq, CAPES and Fundação Araucária for the support. The authors are also grateful to the Foundation for Science and Technology (FCT, Portugal) and FEDER under Programme PT2020 for financial support to CIMO (strategic project UID/AGR/00690/2013) and the research contracts of J. Pinela (Project AllNatt, POCI-01-0145-FEDER-030463) and R. Calhelha. To the project POCI-01-0145-FEDER-006984 – Associate Laboratory LSRE-LCM funded by FEDER through COMPETE2020 - Programa Operacional Competitividade e Internacionalização (POCI) – and by national funds through FCT. This work was also funded by the European Regional Development Fund (ERDF) through the Regional Operational Program North 2020, within the scope of Project NORTE-01-0145-FEDER-023289: DeCodE and Project *Mobilizador* Norte-01-0247-FEDER-024479: ValorNatural®.

Conflicts of interest

There are no conflicts to declare.

References

1 M. Zengin, H. Genc, P. Taslimi, A. Kestane, E. Guclu, A. Ogutlu, O.

View Article Online
DOI: 10.1039/C8FO02431F

Karabay and İ. Gulçin, *Bioorg. Chem.*, 2018, **81**, 119–126.

2 B. Yiğit, M. Yiğit, D. Barut Celepci, Y. Gök, A. Aktaş, M. Aygün, P. Taslimi and İ. Gülçin, *Chem. Sel.*, 2018, **3**, 7976–7982.

3 Q. Li, H. Yang, Y. Chen and H. Sun, *Eur. J. Med. Chem.*, 2017, **132**, 294–309.

4 I. Gülçin, R. Elias, A. Gepdiremen and L. Boyer, *Eur. Food Res. Technol.*, 2006, **223**, 759–767.

5 İ. Gülçin, *Arch. Toxicol.*, 2012, **86**, 345–391.

6 J. E. Klaunig and Z. Wang, *Curr. Opin. Toxicol.*, 2018, **7**, 116–121.

7 I. Batinić-Haberle, J. S. Rebouças and I. Spasojević, *Antioxid. Redox Signal.*, 2010, **13**, 877–918.

8 I. Korovila, M. Hugo, J. P. Castro, D. Weber, A. Höhn, T. Grune and T. Jung, *Redox Biol.*, 2017, **13**, 550–567.

9 G. Tejaswi, M. M. Suchitra, D. Rajasekhar, V. S. Kiranmayi and P. V. L. N. Srinivasa Rao, *J. Indian Coll. Cardiol.*, 2017, **7**, 149–152.

10 S. Chikara, L. D. Nagaprashantha, J. Singhal, D. Horne, S. Awasthi and S. S. Singhal, *Cancer Lett.*, 2018, **413**, 122–134.

11 H. Sies, *Exp. Physiol.*, 1997, **82**, 291–295.

12 C. Ioannides, *Enzyme Systems that Metabolise Drugs and Other Xenobiotics*, John Wiley & Sons, LTD, 2001.

13 M. Schultz, S. Dutta and K. D. Tew, *Adv. Drug Deliv. Rev.*, 1997, **26**, 91–104.

14 H. Soreq and S. Seidman, *Nat. Rev. Neurosci.*, 2001, **2**, 294–302.

View Article Online
DOI: 10.1039/C8FO02431F

15 G. F. d. Sousa, M. G. d. Aguilar, J. A. Takahashi, T. M. A. Alves, M. Kohlhoff, S. A. Vieira Filho, G. D. F. Silva and L. P. Duarte, *Phytochem. Lett.*, 2017, **19**, 34–38.

16 M. L. P. S. Van Iersel, J. P. H. T. M. Ploemen, I. Struik, C. Van Amersfoort, A. E. Keyzer, J. G. Schefferlie and P. J. Van Bladeren, *Chem. Biol. Interact.*, 1996, **102**, 117–132.

17 M. B. Colovic, D. Z. Krstic, T. D. Lazarevic-Pasti, A. M. Bondzic and V. M. Vasic, *Curr. Neuropharmacol.*, 2013, **11**, 315–335.

18 T. Ak and I. Gülçin, *Chem. Biol. Interact.*, 2008, **174**, 27–37.

19 S. K. Bajpai, N. Chand and S. Ahuja, *Int. J. Biol. Macromol.*, 2015, **79**, 440–448.

20 A. C. da Silva, P. D. de F. Santos, N. C. Palazzi, F. V. Leimann, R. H. B. Fuchs, L. Bracht and O. H. Gonçalves, *Food Funct.*, 2017, **8**, 1851–1858.

21 Y. Murakami, H. Ishii, N. Takada, S. Tanaka, M. Machino, S. Ito and S. Fujisawa, *Anticancer Res.*, 2008, **28**, 699–707.

22 B. A. Rocha, O. H. Gonçalves, F. V Leimann, E. S. W. Rebecca, R. A. Silva-buzanello, L. C. Filho, P. H. H. Araújo, R. K. N. Cuman and C. A. Bersani-amado, *Adv. Med. Plant Res.*, 2014, **2**, 62–73.

23 R. M. Srivastava, S. Singh, S. K. Dubey, K. Misra and A. Khar, *Int. Immunopharmacol.*, 2011, **11**, 331–341.

24 P. R. Sarika and R. J. Nirmala, *Mater. Sci. Eng. C*, 2016, **65**, 331–337.

25 T. Ahmed and A. H. Gilani, *Pharmacol. Biochem. Behav.*, 2009, **91**, 554–559.

26 J. A. dos S. Jaques, J. F. P. Rezer, J. F. Gonçalves, R. M. Spanevello, J. M. Gutierres, V. C. Pimentel, G. R. Thomé, V. M. Morsch, M. R. C. Schetinger and D. B. R. Leal, *Cell Biochem. Funct.*, 2011, **29**, 703–707.

27 M. A. Abbasi, M. Ilyas, Aziz-Ur-Rehman, A. Sonia, D. Shahwar, M. A. Raza, K. M. Khan, M. Ashraf, I. Afzal and N. Ambreen, *Sci. Iran.*, 2012, **19**, 1580–1583.

28 P. Sankar, A. G. Telang, R. Kalaivanan, V. Karunakaran, K. Manikam and S. N. Sarkar, *Environ. Toxicol.*, 2013, **30**, 628–637.

29 S. K. Jaiswal, A. Sharma, V. K. Gupta, R. K. Singh and B. Sharma, *Biochem. Res. Int.*, 2016, **2016**, 1–7.

30 Y. Panahi, M. S. Hosseini, N. Khalili, E. Naimi, M. Majeed and A. Sahebkar, *Clin. Nutr.*, 2015, **34**, 1101–1108.

31 S. L. Deng, W. F. Chen, B. Zhou, L. Yang and Z. L. Liu, *Food Chem.*, 2006, **98**, 112–119.

32 J. T. do Prado Silva, J. M. T. Geiss, S. M. Oliveira, E. da S. Brum, S. C. Sagae, D. Becker, F. V. Leimann, R. P. Ineu, G. P. Guerra and O. H. Gonçalves, *Mater. Sci. Eng. C*, 2017, **76**, 1005–1011.

33 J. O. Eloy and J. M. Marchetti, *Powder Technol.*, 2014, **253**, 98–106.

34 E. Karavas, G. Ktistis, A. Xenakis and E. Georgarakis, *Eur. J. Pharm. Biopharm.*, 2006, **63**, 103–114.

35 F. Rocha, L. Yumi Sugahara, F. V. Leimann, S. M. De Oliveira, E. Da Silva Brum, R. C. Calhelha, M. F. Barreiro, I. C. F. R. Ferreira, R. Porto Ineu and O. H. Gonçalves, *Food Funct.*, 2018, **9**, 3698–3706.

View Article Online
DOI: 10.1039/C8FO02431F

36 G. L. Ellman, K. D. Courtney, V. Andres and R. M. Featherstone, *Biochem. Pharmacol.*, 1961, **7**, 88–95.

37 W. H. Habig, M. J. Pabst and W. B. Jakoby, *J. Biol. Chem.*, 1974, **249**, 7130–7139.

38 L. Lockowandt, J. Pinela, C. Lobo, C. Pereira, R. M. V Abreu, R. C. Calhelha, M. José, L. Barros, M. Bredol and I. C. F. R. Ferreira, *Ind. Crop. Prod.*, 2019, **128**, 496–503.

39 B. C. Evans, C. E. Nelson, S. S. Yu, K. R. Beavers, A. J. Kim, H. Li, H. M. Nelson, T. D. Giorgio and C. L. Duvall, *J. Vis. Exp.*, 2013, **73**, 1–5.

40 J. Pinela, L. Barros, A. M. Carvalho and I. C. F. R. Ferreira, *Food Chem. Toxicol.*, 2012, **50**, 829–834.

41 F. Sobral, A. Sampaio, S. Falcão, M. J. R. P. Queiroz, R. C. Calhelha, M. Vilas-Boas and I. C. F. R. Ferreira, *Food Chem. Toxicol.*, , DOI:10.1016/j.fct.2016.06.008.

42 R. M. V Abreu, I. C. F. R. Ferreira, R. C. Calhelha, R. T. Lima, M. H. Vasconcelos, F. Adega, R. Chaves and M. J. R. P. Queiroz, *Eur. J. Med. Chem.*, 2011, **46**, 5800–5806.

43 N. Kaewnopparat, S. Kaewnopparat, A. Jangwang, D. Maneenaun, T. Chuchome and P. Panichayupakaranant, *Int. Sch. Sci. Res. Innov.*, 2009, **3**, 210–215.

44 A. F. Martins, P. V. A. Bueno, E. A. M. S. Almeida, F. H. A. Rodrigues, A. F. Rubira and E. C. Muniz, *Int. J. Biol. Macromol.*, 2013, **57**, 174–184.

45 J. T. do P. Silva, A. C. da Silva, J. M. T. Geiss, P. H. H. de Araújo, D.

View Article Online
DOI: 10.1039/C8FO02431F

Becker, L. Bracht, F. V. Leimann, E. Bona, G. P. Guerra and O. H. Gonçalves, *Food Chem.*, 2017, **230**, 336–342.

46 M. Sampath, R. Lakra and P. Korrapati, *Colloids Surfaces B Biointerfaces*, 2014, **117**, 128–134.

47 S. Raj and D. R. Shankaran, *Sensors Actuators, B Chem.*, 2016, **226**, 318–325.

48 Y. Jafari, H. Sabahi and M. Rahaie, *Food Chem.*, 2016, **211**, 700–706.

49 K. E. Wu, J. Li, W. Wang and D. A. Winstead, 2009, **98**, 2422–2431.

50 K. M. Koczkur, S. Mourdikoudis, L. Polavarapu and S. E. Skrabalak, *Dalt. Trans.*, 2015, **44**, 17883–17905.

51 F. Frizon, J. De Oliveira, C. Maria, M. Lina and J. Maldonado, 2013, **235**, 532–539.

52 A. Paradkar, A. A. Ambike, B. K. Jadhav and K. R. Mahadik, 2004, **271**, 281–286.

53 S. D. Kumavat, Y. S. Chaudhari, P. Borole, K. Shenghani, P. Duvvuri, N. Bubera and P. Shah, *Int. J. Pharm. Res. Sci.*, 2013, **2**, 693–706.

54 W. H. Khan and V. K. Rathod, *Chem. Eng. Process. Process Intensif.*, 2014, **80**, 1–10.

55 J. Li, G. H. Shin, I. W. Lee, X. Chen and H. J. Park, *Food Hydrocoll.*, 2016, **56**, 41–49.

56 A. Catalan-Latorre, M. Ravaghi, M. L. Manca, C. Caddeo, F. Marongiu, G. Ennas, E. Escribano-Ferrer, J. E. Peris, O. Diez-Sales, A. M. Fadda and M. Manconi, *Eur. J. Pharm. Biopharm.*, 2016, **107**, 49–55.

View Article Online
DOI: 10.1039/C8FO02431F

57 K. Siegfried, *Eur. Neuropsychopharmacol.*, 1993, **3**, 170–171.

58 J. A. Araujo, C. M. Studzinski and N. W. Milgram, *Prog. Neuro-Psychopharmacology Biol. Psychiatry*, 2005, **29**, 411–422.

59 R. Hayeshi, I. Mutingwende, W. Mavengere, V. Masiyanise and S. Mukanganyama, *Food Chem. Toxicol.*, 2007, **45**, 286–295.

60 S. Li, C. Li, S. Jin, J. Liu, X. Xue, A. S. Eltahan, J. Sun, J. Tan, J. Dong and X. J. Liang, *Biomaterials*, 2017, **144**, 119–129.

61 S. Oetari, M. Sudibyo, J. N. M. Commandeur, R. Samhoedi and N. P. E. Vermeulen, *Biochem. Pharmacol.*, 1996, **51**, 39–45.

62 A. A. Gorfe, B. Lu, Z. Yu and J. A. McCammon, *Biophys. J.*, 2009, **97**, 897–905.

63 M. A. Prieto and J. A. Vázquez, *Biomed Res. Int.*, 2014, **2014**, 1–15.

64 S. Hatia, A. Septembre-Malaterre, F. Le Sage, A. Badiou-Bénéteau, P. Baret, B. Payet, C. Lefebvre D'hellencourt and M. P. Gonthier, *Free Radic. Res.*, 2014, **48**, 387–401.

65 H. J. Yoon, X. Zhang, M. G. Kang, G. J. Kim, S. Y. Shin, S. H. Baek, B. N. Lee, S. J. Hong, J. T. Kim, K. Hong and H. Bae, *Int. J. Mol. Sci.*, 2018, **19**, 1–12.

66 S. N. H. Zamrus, M. N. Akhtar, S. K. Yeap, C. K. Quah, W. S. Loh, N. B. Alitheen, S. Zareen, S. N. Tajuddin, Y. Hussin and S. A. A. Shah, *Chem. Cent. J.*, 2018, **12**, 1–10.

67 C. C. Chang, C. F. Fu, W. Te Yang, T. Y. Chen and Y. C. Hsu, *Taiwan. J. Obstet. Gynecol.*, 2012, **51**, 368–374.

68 C. Zhao, Y. Cai, X. He, J. Li, L. Zhang, J. Wu, Y. Zhao, S. Yang, X. Li, W. Li and G. Liang, *Eur. J. Med. Chem.*, 2010, **45**, 5773–5780.

Figure 1a

View Article Online
DOI: 10.1039/C8FO02431F

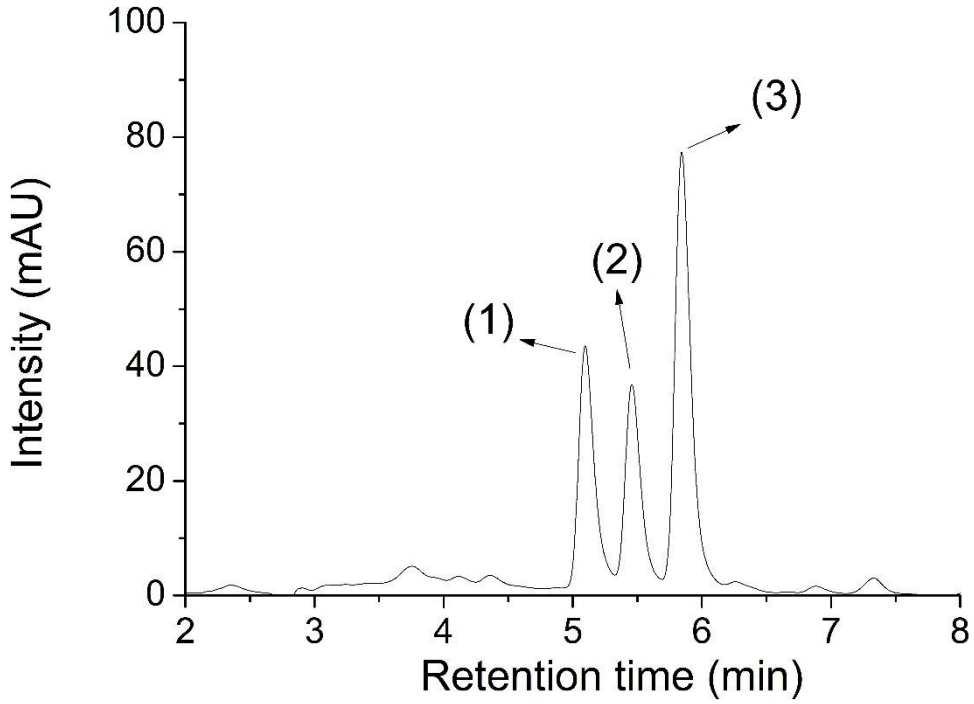

Figure 1b

View Article Online
DOI: 10.1039/C8FO02431F

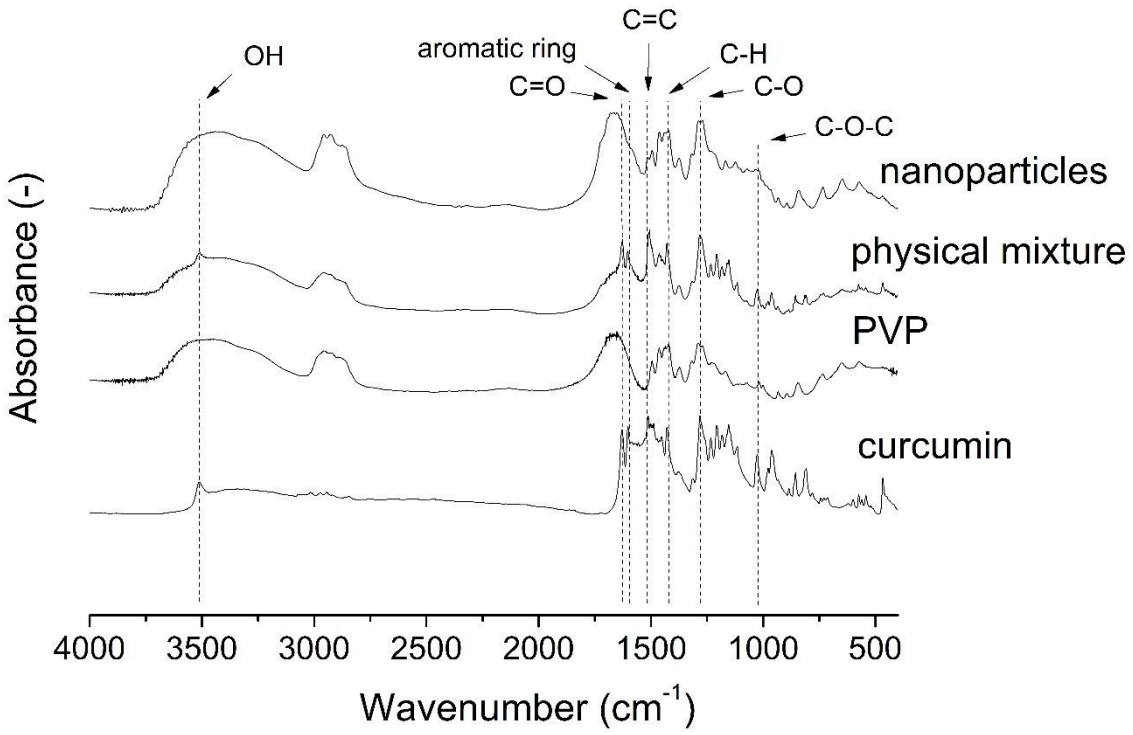

Figure 1c

View Article Online
DOI: 10.1039/C8FO02431F

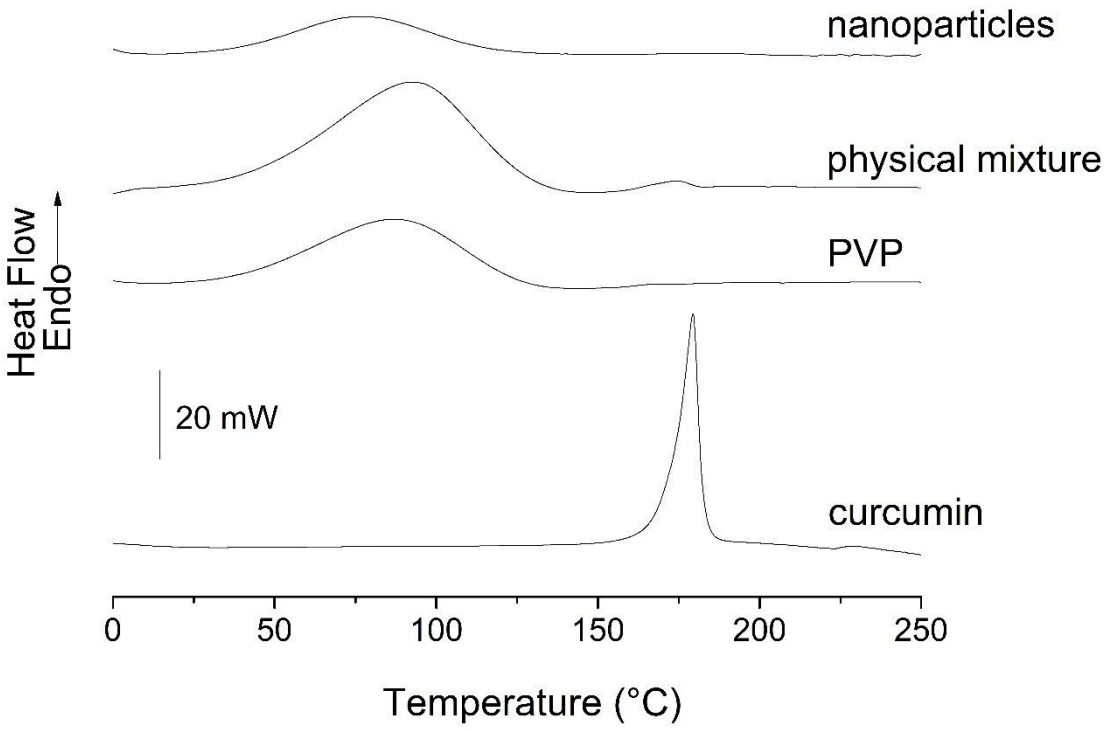

Figure 1d

View Article Online
DOI: 10.1039/C8FO02431F

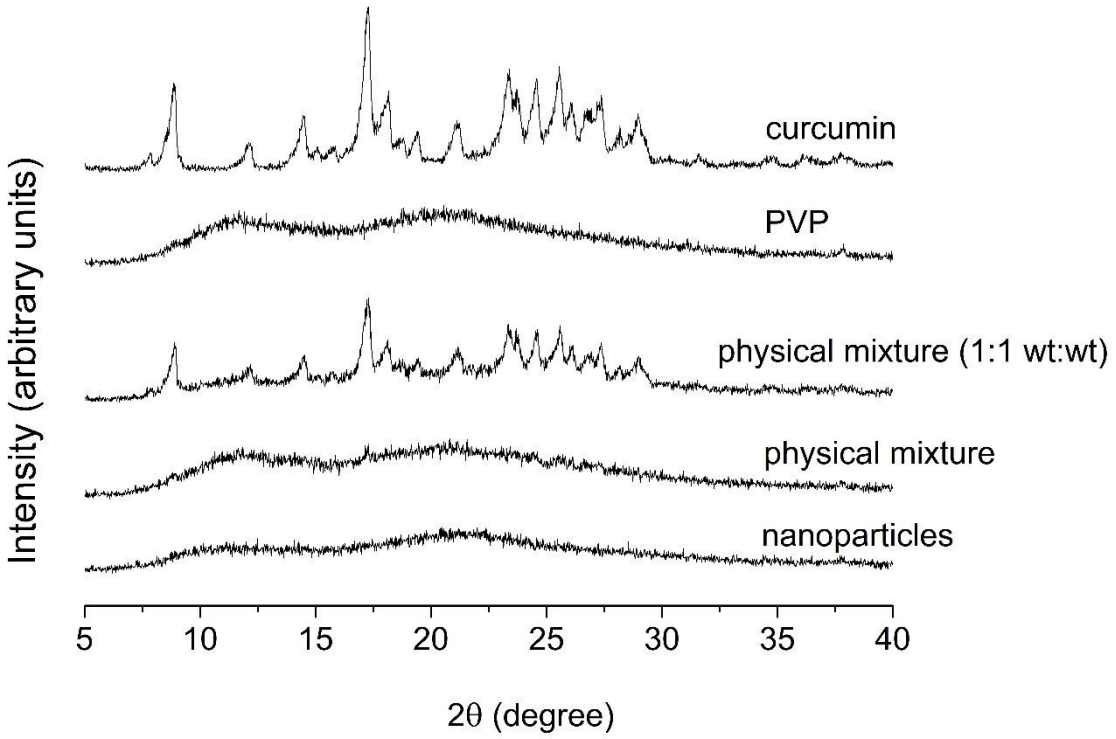

Figure 2

View Article Online
DOI: 10.1039/C8FO02431F

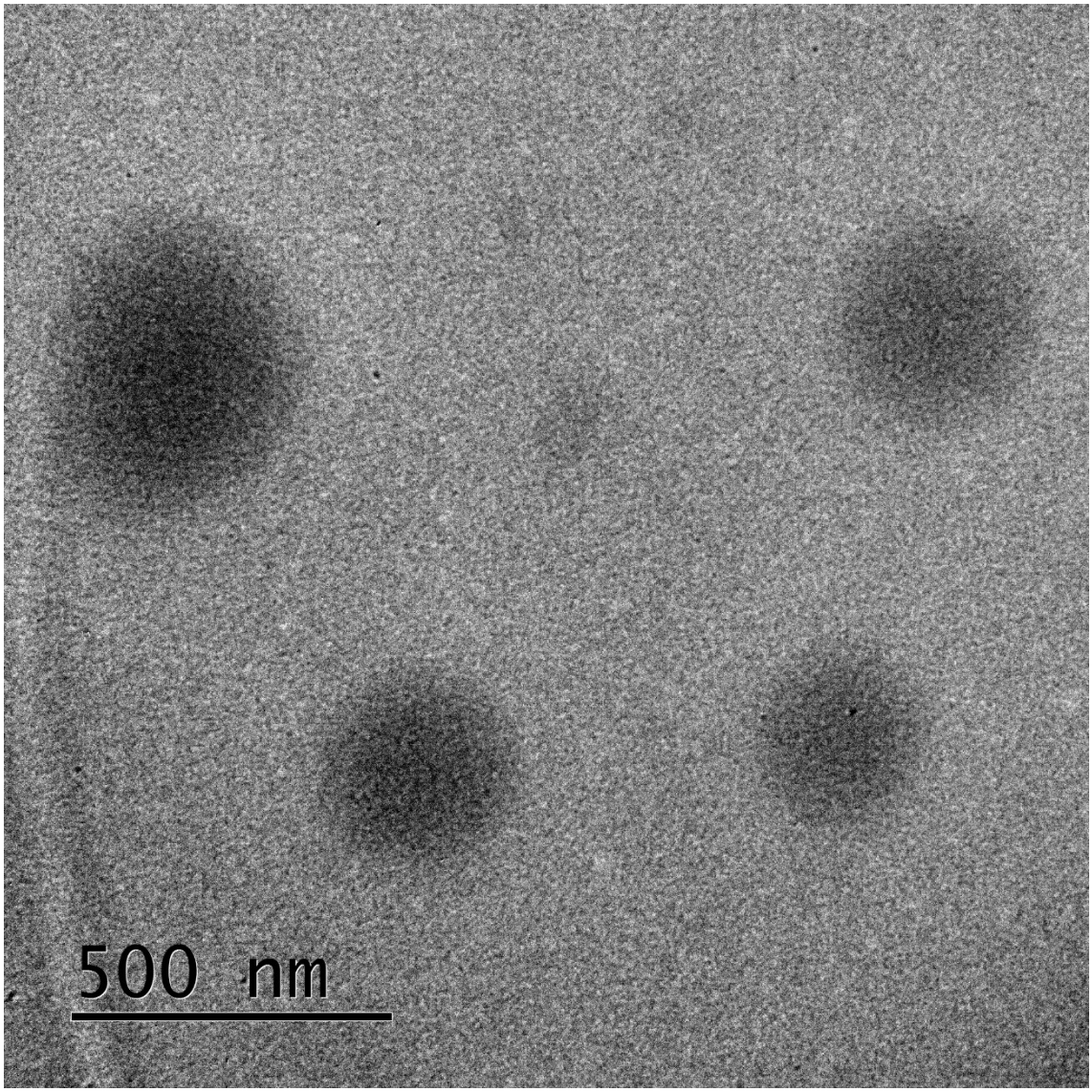

View Article Online
DOI: 10.1039/C8FO02431F

Figure 3a

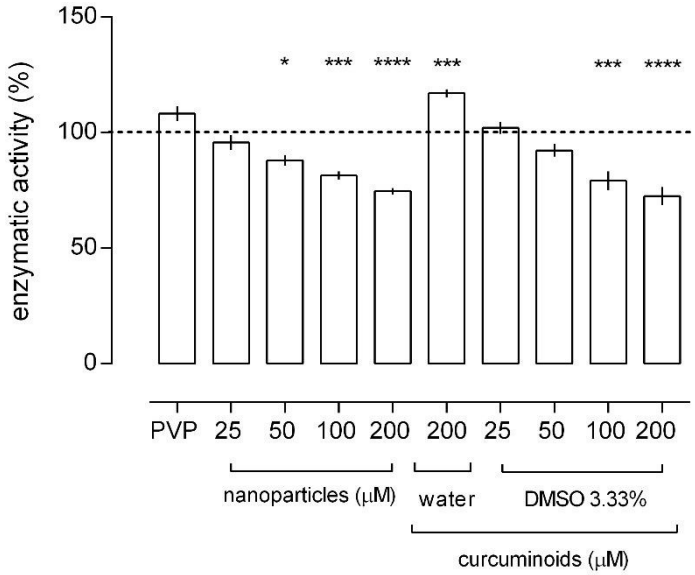

Figure 3b

View Article Online
DOI: 10.1039/C8FO02431F

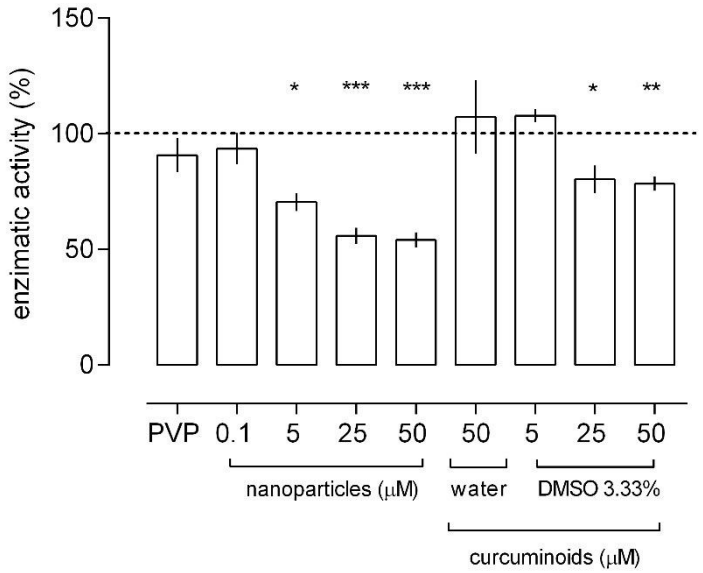

View Article Online
DOI: 10.1039/C8FO02431F

Figure captions

Figure 1. Characterization of the nanoparticles: (a) chromatogram of the curcuminoids nanoparticles (1 - bisdemethoxycurcumin, 2 – demethoxycurcumin and 3 – curcumin); (b) FTIR spectra; (c) DSC thermograms and (d) X-Ray Diffraction patterns. Physical mixtures were obtained at the same curcumin concentration of the nanoparticles (curcumin/PVP ratio of 1:15 wt/wt) and at 1:1 wt:wt when indicated.

Figure 2. Transmission Electron Microscopy image of the curcuminoids nanoparticles.

Figure 3. *In vitro* activity of (a) AChE and (b) GST in the presence of curcuminoids (DMSO 3.33% and water), curcuminoids-loaded nanoparticles (water), and PVP (water). Results represented as mean ± SEM; n = 4. **p* < 0.05; ***p* < 0.01; ****p* < 0.001; *****p* < 0.0001, compared to the control; ††† p < 0.001 between the indicated samples.

Table

Table 1. Antioxidant, anti-inflammatory and cytotoxic activities of free and nanoencapsulated curcuminoids, and positive controls (trolox, dexamethasone or ellipticine).

	Curcuminoids*	**Curcuminoids nanoparticles****	**Positive control**	**Statistics[1]**
Antioxidant activity (IC_{50} values, $\mu g.mL^{-1}$)			Trolox	*p*-value
OxHLIA, Δt = 60 min	7.2 ± 0.5	38.2 ± 0.9	20.1 ± 0.7	<0.001
OxHLIA, Δt = 120 min	15.9 ± 0.4	121 ± 11	44 ± 1	<0.001
TBARS formation inhibition	1.04 ± 0.07	11.9 ± 0.2	5.8 ± 0.6	<0.001
Anti-inflammatory activity (IC_{50} values, $\mu g.mL^{-1}$)			Dexamethasone	
RAW 264.7 (murine macrophages)	61 ± 3	>400	16 ± 1	-
Cytotoxic activity (GI_{50} values, $\mu g.mL^{-1}$)			Ellipticine	
NCI-H460 (non-small cell lung carcinoma)	40 ± 2	344 ± 15	1.03 ± 0.09	<0.001
HeLa (cervical carcinoma)	29 ± 2	315 ± 5	1.91 ± 0.06	<0.001
HepG2 (hepatocellular carcinoma)	23 ± 1	288 ± 14	1.1 ± 0.2	<0.001
MCF-7 (breast carcinoma)	29 ± 1	307 ± 5	1.1 ± 0.2	<0.001
PLP2 (porcine liver primary cells)	101 ± 4	>400	3.2 ± 0.7	-

Results are expressed as mean ± standard deviation.

[1]Statistical differences ($p < 0.05$) among free and nanoencapsulated curcuminoids were assessed by applying a two-tailed paired Student's t-test.

*Curcuminoids dispersed in PBS with 2.5% DMSO for the OxHLIA assay and in DMSO/water mixture (1:1, v/v) for the anti-inflammatory and cytotoxic assays;

**Nanoparticles dispersed in PBS for the OxHLIA assay and in water for the anti-inflammatory and cytotoxic assays.

View Article Online
DOI: 10.1039/C8FO02431F

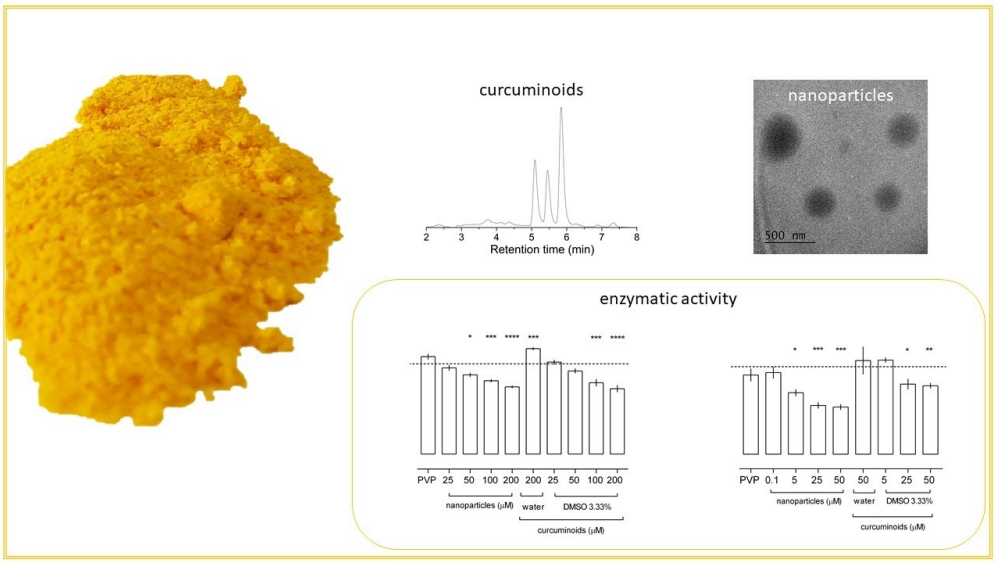

338x190mm (96 x 96 DPI)